PoS PROCEEDINGS OF SCIENCE

Characterization of planar and 3D Silicon pixel sensors for the high luminosity phase of the CMS experiment at LHC

R. Ceccarelli [ab], M. Meschini [a], L. Viliani [a], M. Dinardo [cd], S. Gennai [c], D. Menasce [c], L. Moroni [cd], D. Zuolo* [cd], L. Demaria [e], E. Monteil [e], L. Gaioni [f], A. Messineo [g], E. Currás [h], J. Duarte [h], M. Fernández [h], G. Gómez [h], A. García [h], J. González [h], E. Silva [h], I. Vila [h], G. F. Dalla Betta [i], R. Mendicino [i], M. Boscardin [j]

[a] *INFN Firenze, Italy*
[b] *University of Firenze, Italy*
[c] *INFN Milano Bicocca, Italy*
[d] *University of Milano Bicocca, Italy*
[e] *INFN Torino, Italy*
[f] *INFN Pavia and University of Bergamo, Italy*
[g] *INFN and University of Pisa, Italy*
[h] *IFCA, Spain*
[i] *INFN and University of Trento, Italy*
[j] *FBK - Fondazione Bruno Kessler, Trento, Italy*
E-mail: davide.zuolo@cern.ch

The High Luminosity upgrade of the CERN LHC collider (HL-LHC) demands for a new, high-radiation tolerant solid-state pixel sensor capable of surviving fluencies up to a few 10^{16} n_{eq}/cm^2 at ~ 3 cm from the interaction point. To this extent the INFN ATLAS-CMS joint research activity, in collaboration with Fondazione Bruno Kessler (FBK), is aiming at the development of thin n-in-p type pixel sensors for the HL-LHC. The R&D covers both planar and single-sided 3D columnar pixel devices made with the Si-Si Direct Wafer Bonding technique, which allows for the production of sensors with 100 μm and 130 μm active thickness for planar sensors, and 130 μm for 3D sensors, the thinnest ones ever produced so far. Prototypes of hybrid modules, bump-bonded to the RD53A readout chip, have been tested on beam. First results on their performance before and after irradiation are presented.

European Physical Society Conference on High Energy Physics - EPS-HEP2019 -
10-17 July, 2019
Ghent, Belgium

*Speaker.

© Copyright owned by the author(s) under the terms of the Creative Commons
Attribution-NonCommercial-NoDerivatives 4.0 International License (CC BY-NC-ND 4.0).

PoS(EPS-HEP2019)117

1. Introduction

During its High Luminosity phase, the CERN-LHC collider (HL-LHC) will deliver an instantaneous luminosity of $5 \times 10^{34}\,\mathrm{cm}^{-2}\,\mathrm{s}^{-1}$. After ten years of operation the integrated luminosity will be $\sim 3000\,\mathrm{fb}^{-1}$. The innermost layer of the pixel detector of the CMS experiment, located at $\sim 3\,\mathrm{cm}$ from the interaction point, will be exposed to a fluence of $2.3 \times 10^{16}\,\mathrm{n_{eq}}/\mathrm{cm}^2$. In order to properly operate in such harsh environment new pixel sensors must be developed.

One of the most critical design parameters in the development of these sensors is the distance between the electrodes that generate the electric field inside the cells of the sensor. It is well known that in order to operate these sensors at high irradiation fluences, the input of the pre-amplifier should be connected to the electrode which collects electrons (the faster carriers). Furthermore, in order to keep the bias voltage as low as possible while preserving the largest part of the signal, the distance between opposite sign electrodes should not exceed a few times the electron' mean-free-path at saturation velocity. In our case, at a fluence of $2.3 \times 10^{16}\,n_{eq}/\mathrm{cm}^2$, the electron lifetime becomes $\sim 0.3\,\mathrm{ns}$ and the mean free path at saturated velocity $\sim 30\,\mu\mathrm{m}$. The mean free path of the holes will be even lower, hence their contribution to the signal is lower.

Two different technological solution were available: planar sensors, where the electrodes are parallel to the sensor surface, and 3D sensors, where the electrodes are orthogonal to the sensor surface. In the first case the distance between the electrodes is fixed by the sensor thickness, in the second case the distance is limited by the technological process used to build the sensor.

The INFN ATLAS-CMS joint research activity, in collaboration with Fondazione Bruno Kessler (FBK), developed new thin n-in-p Silicon pixel sensors, employing a recent technology called Direct Wafer Bonding (DWB). Wafers produced using this technology are composed of an underlying p+ type layer with low resistivity and an upper p-type layer with high resistivity, which constitutes the active layer of the sensor [1]. The lower layer provides mechanical support and ohmic contact for the upper layer. Planar sensors are built implanting n+ electrodes on the external surface of the upper layer, as shown in the left-hand side of Figure 1. In the case of 3D sensors, two types of columnar electrodes are implanted: p+ columns, which terminate in the lower layer in order to be biased, and n+ columns, which end $\sim 20\,\mu\mathrm{m}$ before the low resistivity layer as shown in the right-hand side of Figure 1. Two different kinds of 3D sensors are presented here: squared, with pixel dimensions $50 \times 50\,\mu\mathrm{m}^2$, and rectangular, with pixel dimensions $25 \times 100\,\mu\mathrm{m}^2$. Both sensors cells have a n+ electrode in the center and four p+ electrodes at the corners.

Both 3D and planar sensor fabrication processes take place only on one side of the sensor with a consequent reduction of the costs.

Sensors have been bonded to a new read out chip (ROC), named RD53A [2], developed by an ATLAS-CMS collaboration. This ROC features a higher radiation tolerance with respect to the PSI46dig ROC [3], used in our previous test beam campaigns, and can be operated at a much lower threshold (lower than 1500 electrons after irradiation). Cells of this ROC have a dimension of $50 \times 50\,\mu\mathrm{m}^2$.

Three different analog input stages (front-ends), named Synchronous, Linear and Differential, are made available on this first prototype of the Phase-2 pixel ROC for testing purposes. Only results from the linear front-end are reported here.

PoS(EPS-HEP2019)117

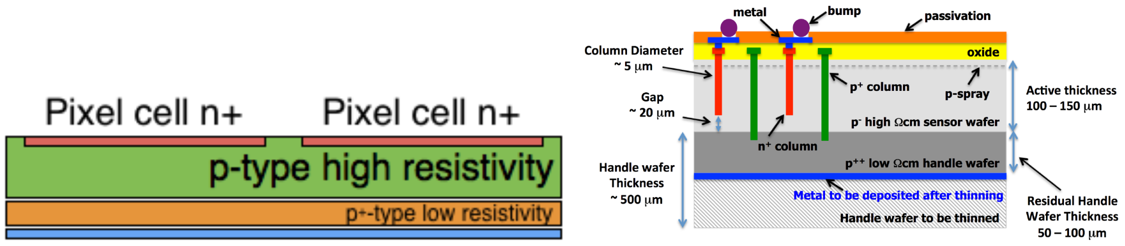

Figure 1: Artistic view of planar (left) and 3D (right) sensors.

Test beam studies of both planar and 3D devices have been performed at three different facilities: Fermilab MTest, using 120 GeV protons; CERN, using 24 GeV protons; and DESY, using 5.2 GeV electrons. First results from test beam campaigns of planar and 3D sensors, both before and after irradiation with protons up to a fluence of $\sim 1 \times 10^{16}\,\mathrm{n_{eq}/cm^2}$, will be presented.

2. Planar Sensors

A planar sensor with $50 \times 50\,\mu\mathrm{m}^2$ pixel cells and 100 μm active thickness has been tested before irradiation at FNAL. The measured Most Probable Value (MPV) of the collected charge is $\sim$ 7300 electrons, which is consistent with the expectations. The measured detection efficiency is greater than 99.7% at a bias voltage of 20 V.

Two planar sensors with $50 \times 50\,\mu\mathrm{m}^2$ pixel cells and 100 μm active thickness have been irradiated at a fluence of $\sim 5 \times 10^{15}\,\mathrm{n_{eq}/cm^2}$ and tested at DESY. The measured detection efficiency is shown on the left-hand side of Figure 2. The module without punch through structures[1] reaches a detection efficiency greater than 99% at a bias voltage of 200 V, while the detection efficiency of the module with punch through structures starts saturating at this bias voltage, reaching a maximum of 97.6% at a bias voltage of 390 V.

Comparing the schematic drawing of four adjacent pixel cells (left-hand side of Figure 3) with the measured detection efficiency of these cells (right-hand side) it is evident that efficiency losses are located in the region of the punch through structure and of its bias grid. The module with punch through structures becomes fully efficient when it is tilted with respect to the direction of the incident particles, as shown on the right-hand side of Figure 2.

3. 3D Sensors

All 3D sensors have an active thickness of 130 μm. The measurements before irradiation already demonstrated that these sensors can reach full performance at bias voltages much lower than those required by the planar sensors of the same active thickness. This is obviously due to the much smaller distance between the electrodes (51.5 μm in the worst case). The MPV of the collected charge is comparable with that of planar sensors with the same active thickness. The

[1] Punch through structures are useful to allow independent testing of the sensor before the bonding to the readout chip.

PoS(EPS-HEP2019)117

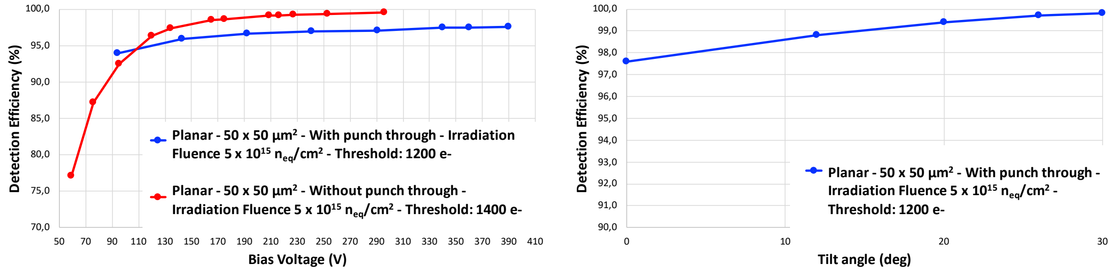

Figure 2: Detection efficiency as a function of the applied bias voltage for the two irradiated planar modules (left) and detection efficiency as a function of the tilt angle for the irradiated planar module with punch through structures (right).

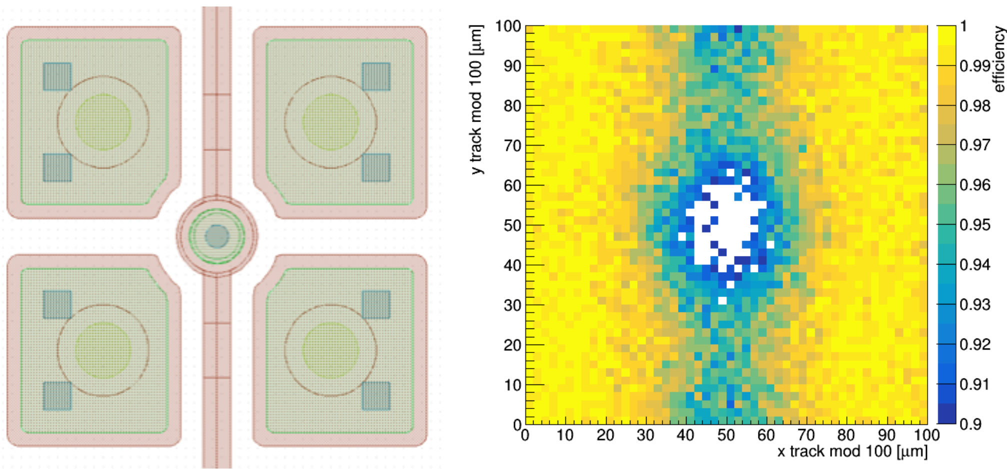

Figure 3: Schematic drawing (left) and map of the detection efficiency (right) of four pixel cells of the planar sensor with punch through structures measured at a bias voltage of 390 V.

detection efficiency is intrinsically limited to $\sim 98.4\%$ by the presence of the electrodes (Figure 1). Full detection efficiency is recovered once the sensors are tilted by a small angle: a rotation of five degrees was sufficient to obtain 99.9 % efficiency.

A sensor with squared pixel cells irradiated at a fluence of $\sim 1 \times 10^{16}\,\mathrm{n_{eq}/cm^2}$ was tested at FNAL. On the left-hand side of Figure 4 the MPV of the collected charge and the detection efficiency measured at FNAL are reported, as a function of the bias voltage: 98% efficiency is reached at a bias voltage of 130 V. This is a very encouraging result since the same efficiency, at the same bias voltage, is reached by the planar sensor irradiated at only half the fluence! On the right-hand side of Figure 4 a map of the cell detection efficiency of this sensor is shown: efficiency losses can be seen in the regions where columnar electrodes are present. Again, when tilting the sensor, such losses are wiped out.

It is important to point out that by selecting a small region in the center of the linear front-end, corresponding to the region that was irradiated with the highest fluence, the measured detection efficiency becomes 97.4%: a very high value considering the level of the irradiation fluence.

PoS(EPS-HEP2019)117

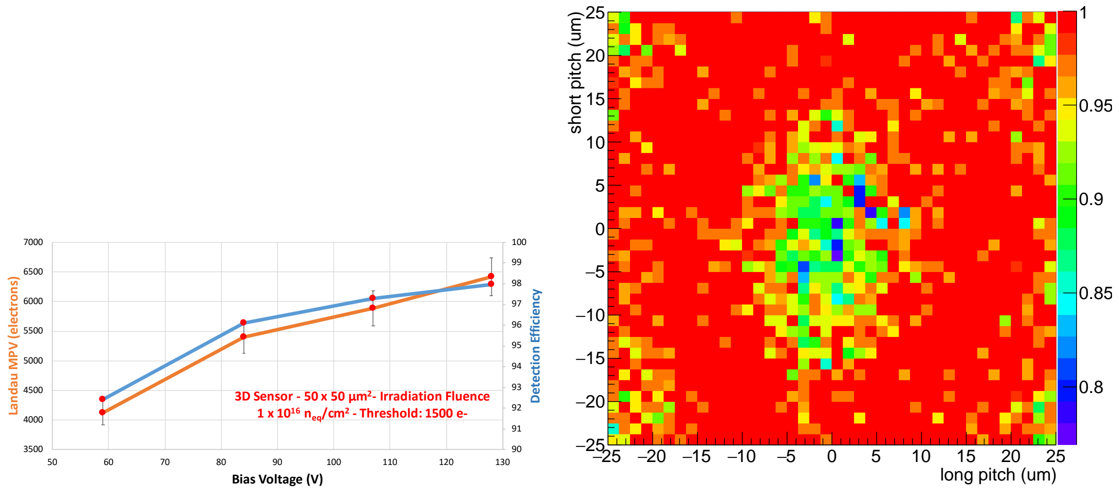

Figure 4: Left: MPV of the collected charge and detection efficiency of a 3D sensor with squared pixels irradiated to a fluence of $\sim 1 \times 10^{16}\,\mathrm{n_{eq}/cm^2}$. Right: cell efficiency map of the same sensor measured at a bias voltage of 180 V.

This sensor was tested also at the CERN test beam facility together with a rectangular sensor ($25 \times 100\,\mu\mathrm{m}^2$) irradiated to the same fluence. The detection efficiency maps of four adjacent cells of the two sensors are reported in Figure 5.

The detection efficiencies of the squared sensor measured at the two test beam facilities are compatible and they are also compatible with the measured efficiency of the rectangular sensor.

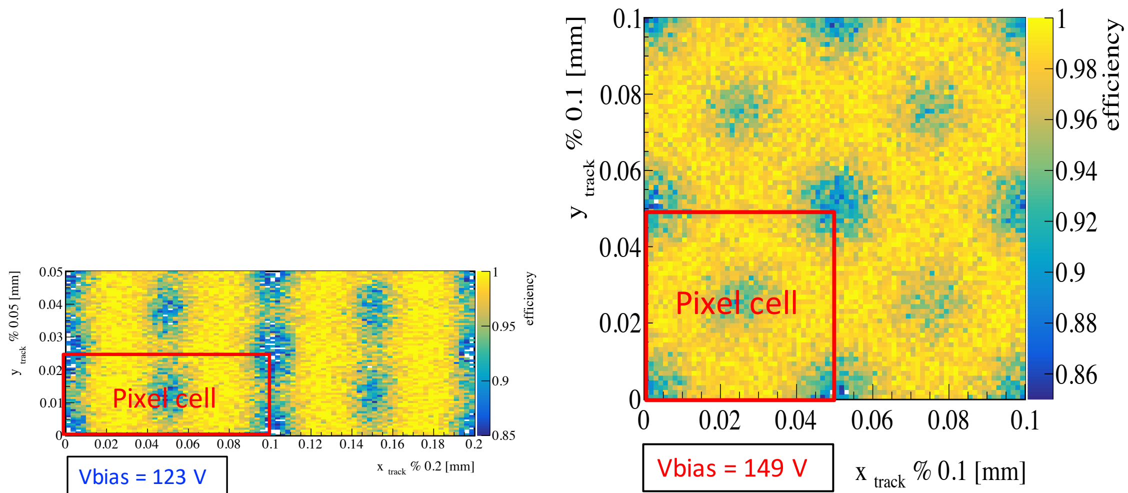

Figure 5: Map of the detection efficiency of four adjacent cells of the 3D sensors with rectangular (left) and squared (right) pixels. Both sensors have been irradiated to a fluence of $\sim 1 \times 10^{16}\,\mathrm{n_{eq}/cm^2}$.

PoS(EPS-HEP2019)117

4. Conclusions

A full characterization of planar and 3D sensors produced with single-sided technology on wafers obtained via Direct Wafer Bonding has been carried out. Measurements after irradiation with protons up to $\sim 5 \times 10^{15}\,\mathrm{n_{eq}/cm^2}$ and $\sim 1 \times 10^{16}\,\mathrm{n_{eq}/cm^2}$, for planar and 3D sensors, respectively, show that these sensors are promising candidates for the Phase-2 upgrade of the inner tracker of the CMS experiment. We are planning new test beam campaigns to test our sensors up to the design fluence expected at the HL-LHC.

Acknowledgments

This work was supported by the Italian National Institute for Nuclear Physics (INFN), Projects ATLAS, CMS, RD-FASE2 (CSN1) and by the H2020 project AIDA-2020, GA no. 654168.

References

[1] IceMos Technology (Belfast, Ireland), http://www.icemostech.com

[2] RD53A ROC Specifications, https://cds.cern.ch/record/2287593

[3] H.C. Kaestli, *Frontend electronics development for the CMS pixel detector upgrade*, *Nucl. Instrum. Meth. A* **731** (2013) 88–91, doi:10.1016/j.nima.2013.05.056.

PoS(EPS-HEP2019)117